

Multi-Task Policy Search

Marc Peter Deisenroth^{1,2}, Peter Englert³, Jan Peters^{2,4}, and Dieter Fox⁵

Abstract—Learning policies that generalize across multiple tasks is an important and challenging research topic in reinforcement learning and robotics. Training individual policies for every single potential task is often impractical, especially for continuous task variations, requiring more principled approaches to share and transfer knowledge among similar tasks. We present a novel approach for learning a nonlinear feedback policy that generalizes across multiple tasks. The key idea is to define a parametrized policy as a function of both the state *and* the task, which allows learning a single policy that generalizes across multiple known and unknown tasks. Applications of our novel approach to reinforcement and imitation learning in real-robot experiments are shown.

I. INTRODUCTION

Complex robots often violate common modeling assumptions, such as rigid-body dynamics. A typical example is a tendon-driven robot arm, shown in Fig. 1, for which these typical assumption are violated due to elasticities and springs. Therefore, learning controllers is a viable alternative to programming robots. To learn controllers for complex robots, reinforcement learning (RL) is promising due to the generality of the RL paradigm [29]. However, without a good initialization (e.g., by human demonstrations [26], [3]) or specific expert knowledge [4] RL often relies on data-intensive learning methods (e.g., Q-learning). For a fragile robotic system, however, thousands of physical interactions are practically infeasible because of time-consuming experiments as well as the wear and tear of the robot.

To make RL practically feasible in robotics, we need to speed up learning by reducing the number of necessary interactions, i.e., robot experiments. For this purpose, model-based RL is often more promising than model-free RL, such as Q-learning or TD-learning [5]. In model-based RL, data is used to learn a model of the system. This model is then used for policy evaluation and improvement, reducing the interaction time with the system. However, model-based RL suffers from *model errors* as it typically assumes that the learned model closely resembles the true underlying dynamics [27], [26]. These model errors propagate through to the learned policy, whose quality inherently depends on the

A concise version of this paper has been published at the *IEEE International Conference on Robotics and Automation (ICRA) 2014* [10].

The research leading to these results has received funding from the European Community's Seventh Framework Programme (FP7/2007-2013) under grant agreement #270327, ONR MURI grant N00014-09-1-1052, and the Department of Computing, Imperial College London.

¹Department of Computing, Imperial College London, UK

²Department of Computer Science, TU Darmstadt, Germany

³Department of Computer Science, University of Stuttgart, Germany

⁴Max Planck Institute for Intelligent Systems, Germany

⁵Department of Computer Science and Engineering, University of Washington, WA, USA

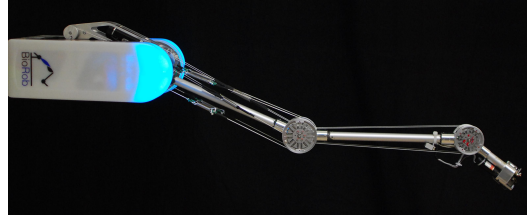


Fig. 1. Tendon-driven BioRob X4.

quality of the learned model. A principled way of accounting for model errors and the resulting optimization bias is to take the uncertainty about the learned model into account for long-term predictions and policy learning [27], [6], [4], [18], [13]. Besides sample-efficient learning for a single task, generalizing learned concepts to new situations is a key research topic in RL. Learned controllers often deal with a single situation/context, e.g., they drive the system to a desired state. In a robotics context, solutions for multiple related tasks are often desired, e.g., for grasping multiple objects [21] or in robot games, such as learning hitting movements in table tennis [22], or in generalizing kicking movements in robot soccer [7].

Unlike most other multi-task scenarios, we consider a set-up with a continuous set of tasks η . The objective is to learn a policy that is capable of solving related tasks in the prescribed class. Since it is often impossible to learn individual policies for all conceivable tasks, a multi-task learning approach is required that can generalize across these tasks. We assume that during *training*, i.e., policy learning, the robot is given a small set of training tasks η_i^{train} . In the *test phase*, the learned policy is expected to generalize from the training tasks to previously unseen, but related, test tasks η_i^{test} .

Two general approaches exist to tackle this challenge by either hierarchically combining local controllers or a richer policy parametrization. First, local policies can be learned, and, subsequently, generalization can be achieved by combining them, e.g., by means of a gating network [17]. This approach has been successfully applied in RL [30] and robotics [22]. In [22] a gating network is used to generalize a set of motor primitives for hitting movements in robot-table tennis. The limitation of this approach is that it can only deal with convex combinations of local policies, implicitly requiring local policies that are linear in the policy parameters.¹ In [31], [7], it was proposed to share state-action

¹One way of making hierarchical models more flexible is to learn the hierarchy jointly with the local controllers. To the best of our knowledge, such a solution does not exist yet.

values across tasks to transfer knowledge. This approach was successfully applied to kicking a ball with a NAO robot in the context of RoboCup. However, a mapping from source to target tasks is explicitly required. In [8], it is proposed to sample a number of tasks from a task distribution, learn the corresponding individual policies, and generalize them to new problems by combining classifiers and nonlinear regression. In [19], [8] it is proposed to learn mappings from tasks to meta-parameters of a policy to generalize across tasks. The task-specific policies are trained independently, and the elementary movements are given by Dynamic Movement Primitives [16]. Second, instead of learning local policies one can parametrize the policy directly by the task. For instance, in [20], a value function-based transfer learning approach is proposed that generalizes across tasks by finding a regression function mapping a task-augmented state space to expected returns. We follow this second approach since it allows for generalizing nonlinear policies: During training, access to a set of tasks is given and a *single* controller is learned jointly for all tasks using policy search. Generalization to unseen tasks in the same domain is achieved by defining the policy as a function of both the state and the task. At test time, this allows for generalization to unseen tasks *without* retraining, which often cannot be done in real time. For learning the parameters of the multi-task policy, we use the PILCO policy search framework [11]. PILCO learns flexible Gaussian process (GP) forward models and uses fast deterministic approximate inference for long-term predictions to achieve data-efficient learning. In a robotics context, policy search methods have been successfully applied to many tasks [12] and seem to be more promising than value function-based methods for learning policies. Hence, this paper addresses two key problems in robotics: multi-task and data-efficient policy learning.

II. POLICY SEARCH FOR LEARNING MULTIPLE TASKS

We consider dynamical systems $\mathbf{x}_{t+1} = f(\mathbf{x}_t, \mathbf{u}_t) + \mathbf{w}$ with continuous states $\mathbf{x} \in \mathbb{R}^D$ and controls $\mathbf{u} \in \mathbb{R}^F$ and unknown transition dynamics f . The term $\mathbf{w} \sim \mathcal{N}(\mathbf{0}, \Sigma_w)$ is zero-mean i.i.d. Gaussian noise with covariance matrix Σ_w . In (single-task) policy search, our objective is to find a deterministic *policy* $\pi : \mathbf{x} \mapsto \pi(\mathbf{x}, \boldsymbol{\theta}) = \mathbf{u}$ that minimizes the *expected long-term cost*

$$J^\pi(\boldsymbol{\theta}) = \sum_{t=1}^T \mathbb{E}_{\mathbf{x}_t} [c(\mathbf{x}_t)], \quad p(\mathbf{x}_0) = \mathcal{N}(\boldsymbol{\mu}_0^x, \Sigma_0^x), \quad (1)$$

of following π for T steps. Note that the trajectory $\mathbf{x}_1, \dots, \mathbf{x}_T$ depends on the policy π and, thus, the parameters $\boldsymbol{\theta}$. In Eq. (1), $c(\mathbf{x}_t)$ is a given cost function of state \mathbf{x} at time t . The policy π is parametrized by $\boldsymbol{\theta} \in \mathbb{R}^P$. Typically, the cost function c incorporates some information about a task $\boldsymbol{\eta}$, e.g., a desired target location $\mathbf{x}_{\text{target}}$ or a trajectory. Finding a policy that minimizes Eq. (1) solves the task $\boldsymbol{\eta}$ of controlling the robot toward the target.

A. Task-Dependent Policies

We propose to learn a *single* policy for all tasks jointly to generalize classical policy search to a multi-task scenario. We

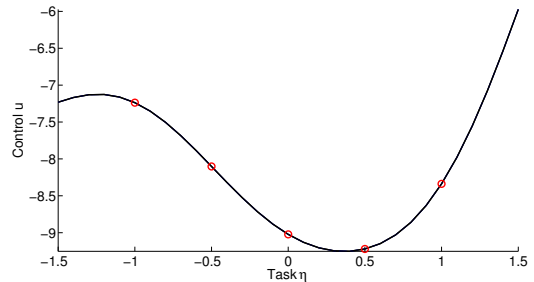


Fig. 2. Generalization ability of a multi-task policy for the cart-pole experiment in Sec. III-A. Here, the state is fixed, the change in the controls is solely due to the change in the task. The black line represents the corresponding policy that has been augmented with the task. The controls of the training tasks are denoted by the red circles. The policy smoothly generalizes across test tasks.

assume that the dynamics are stationary with the transition probabilities and control spaces shared by all tasks. By learning a single policy that is sufficiently flexible to learn the training tasks $\boldsymbol{\eta}_i^{\text{train}}$, we aim to obtain good generalization performance to related test tasks $\boldsymbol{\eta}_j^{\text{test}}$ by reducing the danger of overfitting to the training tasks, a common problem with current hierarchical approaches.

To learn a single controller for multiple tasks $\boldsymbol{\eta}_k$, we propose to make the policy a function of the state \mathbf{x} , the parameters $\boldsymbol{\theta}$, and the task $\boldsymbol{\eta}$, such that $\mathbf{u} = \pi(\mathbf{x}, \boldsymbol{\eta}, \boldsymbol{\theta})$. In this way, a trained policy has the potential to generalize to previously unseen tasks by computing different control signals for a fixed state \mathbf{x} and parameters $\boldsymbol{\theta}$ but varying tasks $\boldsymbol{\eta}_k$. Fig. 2 gives an intuition of what kind of generalization power we can expect from a policy that uses state-task pairs as inputs: Assume a given policy parametrization, a fixed state, and five training targets $\boldsymbol{\eta}_i^{\text{train}}$. For each pair $(\mathbf{x}, \boldsymbol{\eta}_i^{\text{train}}, \boldsymbol{\theta})$, the policy determines the corresponding controls $\pi(\mathbf{x}, \boldsymbol{\eta}_i^{\text{train}}, \boldsymbol{\theta})$, which are denoted by the red circles. The differences in these control signals are achieved solely by changing $\boldsymbol{\eta}_i^{\text{train}}$ in $\pi(\mathbf{x}, \boldsymbol{\eta}_i^{\text{train}}, \boldsymbol{\theta})$ as \mathbf{x} and $\boldsymbol{\theta}$ were assumed fixed. The parametrization of the policy by $\boldsymbol{\theta}$ and $\boldsymbol{\eta}$ implicitly determines the generalization power of π to new (but related) tasks $\boldsymbol{\eta}_j^{\text{test}}$ at test time. The policy for a fixed state but varying test tasks $\boldsymbol{\eta}_j^{\text{test}}$ is represented by the black curve. To find good parameters of the multi-task policy, we incorporate our multi-task learning approach into the model-based PILCO policy search framework [13]. The high-level steps of the resulting algorithm are summarized in Fig. 3. We assume that a set of training tasks $\boldsymbol{\eta}_i^{\text{train}}$ is given. The parametrized policy π is initialized randomly and, subsequently, applied to the robot, see line 1 in Fig. 3. Based on the initial collected data, a probabilistic GP forward model of the underlying robot dynamics is learned (line 3) to consistently account for model errors [25].

We define the policy π as an explicit function of both the state \mathbf{x} and the task $\boldsymbol{\eta}$, which essentially means that the policy depends on a task-augmented state and $\mathbf{u} = \pi(\mathbf{x}, \boldsymbol{\eta}, \boldsymbol{\theta})$. Before going into detail, let us consider the case where a function g relates state and task. In this paper, we consider two cases: (a) A linear relationship between

Fig. 3. Multi-Task Policy Search

- 1: **init:** Pass in training tasks η_i^{train} , initialize policy parameters θ randomly. Apply random control signals and record data.
- 2: **repeat**
- 3: Update GP forward dynamics model using all data
- 4: **repeat**
- 5: Long-term predictions: Compute $\mathbb{E}_\eta[J^\pi(\theta, \eta)]$
- 6: Analytically compute gradient $\mathbb{E}_\eta[dJ^\pi(\theta, \eta)/d\theta]$
- 7: Update policy parameters θ (e.g., BFGS)
- 8: **until** convergence; **return** θ^*
- 9: Set $\pi^* \leftarrow \pi(\theta^*)$
- 10: Apply π^* to robot and record data
- 11: **until** $\forall i$: task η_i^{train} learned
- 12: Apply π^* to test tasks η_j^{test}

the task η and the state \mathbf{x}_t with $g(\mathbf{x}_t, \eta) = \eta - \mathbf{x}_t$. For example, the state and the task (corresponding to a target location) can be both defined in camera coordinates, and the target location parametrizes and defines the task. (b) The task variable η and the state vector are not directly related, in which case $g(\mathbf{x}_t, \eta) = \eta$. For instance, the task variable could simply be an index. We approximate the joint distribution $p(\mathbf{x}_t, g(\mathbf{x}_t, \eta))$ by a Gaussian

$$\mathcal{N}\left(\begin{bmatrix} \boldsymbol{\mu}_t^x \\ \boldsymbol{\mu}_t^\eta \end{bmatrix}, \begin{bmatrix} \boldsymbol{\Sigma}_t^x & \mathbf{C}_t^{x\eta} \\ \mathbf{C}_t^{\eta x} & \boldsymbol{\Sigma}_t^\eta \end{bmatrix}\right) =: \mathcal{N}(\mathbf{x}_t^{x,\eta} | \boldsymbol{\mu}_t^{x,\eta}, \boldsymbol{\Sigma}_t^{x,\eta}), \quad (2)$$

where the state distribution is $\mathcal{N}(\mathbf{x}_t | \boldsymbol{\mu}_t^x, \boldsymbol{\Sigma}_t^x)$ and $\mathbf{C}_t^{x\eta}$ is the cross-covariance between the state and $g(\mathbf{x}_t, \eta)$. The cross-covariances for $g(\mathbf{x}_t, \eta) = \eta - \mathbf{x}_t$ are $\mathbf{C}_t^{x\eta} = -\boldsymbol{\Sigma}_t^x$. If the state and the task are not directly related, i.e., $g(\mathbf{x}_t, \eta) = \eta$, then $\mathbf{C}_t^{x\eta} = \mathbf{0}$.

The Gaussian approximation of the joint distribution $p(\mathbf{x}_t, g(\mathbf{x}_t, \eta))$ in Eq. (2) serves as the input distribution to the controller function π . Although we assume that the tasks η_i^{test} are given deterministically at test time, introducing a task uncertainty $\boldsymbol{\Sigma}_t^\eta > \mathbf{0}$ during *training* can make sense for two reasons: First, during *training* $\boldsymbol{\Sigma}_t^\eta$ defines a *task distribution*, which may allow for better generalization performance compared to $\boldsymbol{\Sigma}_t^\eta = \mathbf{0}$. Second, $\boldsymbol{\Sigma}_t^\eta > \mathbf{0}$ induces uncertainty into planning and policy learning. Therefore, $\boldsymbol{\Sigma}_t^\eta$ serves as a regularizer and makes policy overfitting less likely.

B. Multi-Task Policy Evaluation

For policy evaluation, we analytically approximate the expected long-term cost $J^\pi(\theta)$ by averaging over all tasks η , see line 5 in Fig. 3, according to

$$\mathbb{E}_\eta[J^\pi(\theta, \eta)] \approx \frac{1}{M} \sum_{i=1}^M J^\pi(\theta, \eta_i^{\text{train}}), \quad (3)$$

where M is the number of tasks considered during training. The expected cost $J^\pi(\theta, \eta_i^{\text{train}})$ corresponds to Eq. (1) for a specific training task η_i^{train} . The intuition behind the expected long-term cost in Eq. (3) is to allow for learning a single controller for multiple tasks *jointly*. Hence, the controller

parameters θ have to be updated in the context of *all* tasks. The resulting controller is not necessarily optimal for a *single* task, but (neglecting approximations and local minima) optimal across *all tasks* on average, presumably leading to good generalization performance. The expected long-term cost $J^\pi(\theta, \eta_i^{\text{train}})$ in Eq. (3) is computed as follows.

First, based on the learned GP dynamics model, approximations to the long-term predictive state distributions $p(\mathbf{x}_1 | \eta), \dots, p(\mathbf{x}_T | \eta)$ are computed analytically: Given a joint Gaussian prior distribution $p(\mathbf{x}_t, \mathbf{u}_t | \eta)$, the distribution of the successor state

$$p(\mathbf{x}_{t+1} | \eta_i^{\text{train}}) = \iiint p(\mathbf{x}_{t+1} | \mathbf{x}_t, \mathbf{u}_t) p(\mathbf{x}_t, \mathbf{u}_t | \eta_i^{\text{train}}) d\mathbf{x}_t d\mathbf{u}_t \quad (4)$$

cannot be computed analytically for nonlinear covariance functions. However, we approximate it by a Gaussian distribution $\mathcal{N}(\mathbf{x}_{t+1} | \boldsymbol{\mu}_{t+1}^x, \boldsymbol{\Sigma}_{t+1}^x)$ using exact moment matching [24], [11]. In Eq. (4), the transition probability $p(\mathbf{x}_{t+1} | \mathbf{x}_t, \mathbf{u}_t) = p(f(\mathbf{x}_t, \mathbf{u}_t) | \mathbf{x}_t, \mathbf{u}_t)$ is the GP predictive distribution at $(\mathbf{x}_t, \mathbf{u}_t)$. Iterating the moment-matching approximation of Eq. (4) for all time steps of the finite horizon T yields Gaussian marginal predictive distributions $p(\mathbf{x}_1 | \eta_i^{\text{train}}), \dots, p(\mathbf{x}_T | \eta_i^{\text{train}})$.

Second, these approximate Gaussian long-term predictive state distributions allow for the computation of the expected immediate cost $\mathbb{E}_{\mathbf{x}_t}[c(\mathbf{x}_t) | \eta_i^{\text{train}}] = \int c_\eta(\mathbf{x}_t) p(\mathbf{x}_t | \eta_i^{\text{train}}) d\mathbf{x}_t$ for a particular task η_i^{train} , where $p(\mathbf{x}_t | \eta_i^{\text{train}}) = \mathcal{N}(\mathbf{x}_t | \boldsymbol{\mu}_t^x, \boldsymbol{\Sigma}_t^x)$ and c_η is a task-specific cost function. This integral can be solved analytically for many choices of the immediate cost function c_η , such as polynomials, trigonometric functions, or unnormalized Gaussians. Summing the values $\mathbb{E}_{\mathbf{x}_t}[c(\mathbf{x}_t) | \eta_i^{\text{train}}]$ from $t = 1, \dots, T$ finally yields $J^\pi(\theta, \eta_i^{\text{train}})$ in Eq. (3).

C. Gradient-based Policy Improvement

The deterministic and analytic approximation of $J^\pi(\theta, \eta)$ by means of moment matching allows for an analytic computation of the corresponding gradient $dJ^\pi(\theta, \eta)/d\theta$ with respect to the policy parameters θ , see Eq. (3) and line 6 in Fig. 3, which are given by

$$\frac{dJ^\pi(\theta, \eta)}{d\theta} = \sum_{t=1}^T \frac{d}{d\theta} \mathbb{E}_{\mathbf{x}_t}[c(\mathbf{x}_t) | \eta]. \quad (5)$$

These gradients can be used in any gradient-based optimization toolbox, e.g., BFGS (line 7). Analytic computation of $J^\pi(\theta, \eta)$ and its gradients $dJ^\pi(\theta, \eta)/d\theta$ is more efficient than estimating policy gradients through sampling: For the latter, the variance in the gradient estimate grows quickly with the number of policy parameters and the horizon T [23].

Computing the derivatives of $J^\pi(\theta, \eta_i^{\text{train}})$ with respect to the policy parameters θ requires repeated application of the chain-rule. Defining $\mathcal{E}_t := \mathbb{E}_{\mathbf{x}_t}[c(\mathbf{x}_t) | \eta_i^{\text{train}}]$ in Eq. (5) yields

$$\frac{d\mathcal{E}_t}{d\theta} = \frac{d\mathcal{E}_t}{dp(\mathbf{x}_t)} \frac{dp(\mathbf{x}_t)}{d\theta} := \frac{\partial \mathcal{E}_t}{\partial \boldsymbol{\mu}_t^x} \frac{d\boldsymbol{\mu}_t^x}{d\theta} + \frac{\partial \mathcal{E}_t}{\partial \boldsymbol{\Sigma}_t^x} \frac{d\boldsymbol{\Sigma}_t^x}{d\theta}, \quad (6)$$

where we took the derivative with respect to $p(\mathbf{x}_t)$, i.e., the parameters of the state distribution $p(\mathbf{x}_t)$. In Eq. (6), this

amounts to computing the derivatives of \mathcal{E}_t with respect to the mean $\boldsymbol{\mu}_t^x$ and covariance $\boldsymbol{\Sigma}_t^x$ of the Gaussian approximation of $p(\mathbf{x}_t)$. The chain-rule yields the total derivative of $p(\mathbf{x}_t)$ with respect to $\boldsymbol{\theta}$

$$\frac{dp(\mathbf{x}_t)}{d\boldsymbol{\theta}} = \frac{\partial p(\mathbf{x}_t)}{\partial p(\mathbf{x}_{t-1})} \frac{dp(\mathbf{x}_{t-1})}{d\boldsymbol{\theta}} + \frac{\partial p(\mathbf{x}_t)}{\partial \boldsymbol{\theta}}. \quad (7)$$

In Eq. (7), we assume that the total derivative $dp(\mathbf{x}_{t-1})/d\boldsymbol{\theta}$ is known from the computation for the previous time step. Hence, we only need to compute the partial derivative $\partial p(\mathbf{x}_t)/\partial \boldsymbol{\theta}$. Note that $\mathbf{x}_t = f(\mathbf{x}_{t-1}, \mathbf{u}_{t-1}) + \mathbf{w}$ and $\mathbf{u}_{t-1} = \pi(\mathbf{x}_{t-1}, g(\mathbf{x}_{t-1}, \boldsymbol{\eta}), \boldsymbol{\theta})$. Therefore, with the Gaussian approximation to the marginal state distribution $p(\mathbf{x}_t)$, $\partial p(\mathbf{x}_t)/\partial \boldsymbol{\theta} = \{\partial \boldsymbol{\mu}_t^x/\partial \boldsymbol{\theta}, \partial \boldsymbol{\Sigma}_t^x/\partial \boldsymbol{\theta}\}$ with

$$\begin{aligned} \frac{\partial \{\boldsymbol{\mu}_t^x, \boldsymbol{\Sigma}_t^x\}}{\partial \boldsymbol{\theta}} &= \frac{\partial \{\boldsymbol{\mu}_t^x, \boldsymbol{\Sigma}_t^x\}}{\partial p(\mathbf{u}_{t-1})} \frac{\partial p(\mathbf{u}_{t-1})}{\partial \boldsymbol{\theta}} \\ &= \frac{\partial \{\boldsymbol{\mu}_t^x, \boldsymbol{\Sigma}_t^x\}}{\partial \boldsymbol{\mu}_{t-1}^u} \frac{\partial \boldsymbol{\mu}_{t-1}^u}{\partial \boldsymbol{\theta}} + \frac{\partial \{\boldsymbol{\mu}_t^x, \boldsymbol{\Sigma}_t^x\}}{\partial \boldsymbol{\Sigma}_{t-1}^u} \frac{\partial \boldsymbol{\Sigma}_{t-1}^u}{\partial \boldsymbol{\theta}}. \end{aligned} \quad (8)$$

Here, the distribution

$$p(\mathbf{u}_{t-1}) = \int \pi(\mathbf{x}_{t-1}, g(\mathbf{x}_{t-1}, \boldsymbol{\eta}), \boldsymbol{\theta}) p(\mathbf{x}_{t-1}) d\mathbf{x}_{t-1}$$

of the control signal is approximated by a Gaussian with mean $\boldsymbol{\mu}_{t-1}^u$ and covariance $\boldsymbol{\Sigma}_{t-1}^u$. These moments (and their gradients with respect to $\boldsymbol{\theta}$) can often be computed analytically, e.g., in linear models with polynomial or Gaussian basis functions. The augmentation of the policy with the (transformed) task variable requires an additional layer of gradients for computing $dJ^\pi(\boldsymbol{\theta})/d\boldsymbol{\theta}$. The variable transformation affects the partial derivatives of $\boldsymbol{\mu}_{t-1}^u$ and $\boldsymbol{\Sigma}_{t-1}^u$ (marked red in Eq. (8)), such that

$$\begin{aligned} \frac{\partial \{\boldsymbol{\mu}_{t-1}^u, \boldsymbol{\Sigma}_{t-1}^u\}}{\partial \{\boldsymbol{\mu}_{t-1}^x, \boldsymbol{\Sigma}_{t-1}^x, \boldsymbol{\theta}\}} &= \frac{\partial \{\boldsymbol{\mu}_{t-1}^u, \boldsymbol{\Sigma}_{t-1}^u\}}{\partial p(\mathbf{x}_{t-1}, g(\mathbf{x}_{t-1}, \boldsymbol{\eta}))} \\ &\quad \times \frac{\partial p(\mathbf{x}_{t-1}, g(\mathbf{x}_{t-1}, \boldsymbol{\eta}))}{\partial \{\boldsymbol{\mu}_{t-1}^x, \boldsymbol{\Sigma}_{t-1}^x, \boldsymbol{\theta}\}}, \end{aligned} \quad (9)$$

which can often be computed analytically. Similar to [11], we combine these derivatives with the gradients in Eq. (8) via the chain and product-rules, yielding an analytic gradient $dJ^\pi(\boldsymbol{\theta}, \boldsymbol{\eta}_i^{\text{train}})/d\boldsymbol{\theta}$ in Eq. (3), which is used for gradient-based policy updates, see lines 6–7 in Fig. 3.

III. EVALUATIONS AND RESULTS

In the following, we analyze our approach to multi-task policy search on three scenarios: 1) the under-actuated cart-pole swing-up benchmark, 2) a low-cost robotic manipulator system that learns block stacking, and 3) an imitation learning ball-hitting task with a tendon-driven robot. In all cases, the system dynamics were unknown and inferred from data using GPs.

A. Multi-Task Cart-Pole Swing-up

We applied our proposed multi-task policy search to learning a model and a controller for the cart-pole swing-up. The system consists of a cart with mass 0.5 kg and a pendulum of length 0.6 m and mass 0.5 kg attached to

the cart. Every 0.1 s, an external force was applied to the cart, but not to the pendulum. The friction between cart and ground was 0.1 Ns/m. The state $\mathbf{x} = [\chi, \dot{\chi}, \varphi, \dot{\varphi}]$ of the system comprised the position χ of the cart, the velocity $\dot{\chi}$ of the cart, the angle φ of the pendulum, and the angular velocity $\dot{\varphi}$ of the pendulum. For the equations of motion, we refer to [9]. The nonlinear controller was parametrized as a regularized RBF network with 100 Gaussian basis functions. The controller parameters were the locations of the basis functions, a shared (diagonal) width-matrix, and the weights, resulting in approximately 800 policy parameters.

Initially, the system was expected to be in a state, where the pendulum hangs down; more specifically, $p(\mathbf{x}_0) = \mathcal{N}(\mathbf{0}, 0.1^2 \mathbf{I})$. By pushing the cart to the left and to the right, the objective was to swing the pendulum up and to balance it in the inverted position at a target location $\boldsymbol{\eta}$ of the cart specified at *test time*, such that $\mathbf{x}_{\text{target}} = [\boldsymbol{\eta}, *, \pi + 2k\pi, *]$ with $\boldsymbol{\eta} \in [-1.5, 1.5]$ m and $k \in \mathbb{Z}$. The cost function c in Eq. (1) was chosen as $c(\mathbf{x}) = 1 - \exp(-8\|\mathbf{x} - \mathbf{x}_{\text{target}}\|^2) \in [0, 1]$ and penalized the Euclidean distance of the tip of the pendulum from its desired inverted position with the cart being at target location $\boldsymbol{\eta}$. Optimally solving the task required the cart to stop at the target location $\boldsymbol{\eta}$. Balancing the pendulum with the cart offset by 20 cm caused an immediate cost (per time step) of about 0.4. We considered four experimental setups: **Nearest neighbor independent controllers (NN-IC)**: Nearest-neighbor baseline experiment with five independently learned controllers for the desired swing-up locations $\boldsymbol{\eta} = \{\pm 1 \text{ m}, \pm 0.5 \text{ m}, 0 \text{ m}\}$. Each controller was learned using the PILCO framework [13] in 10 trials with a total experience of 200 s. For the test tasks $\boldsymbol{\eta}^{\text{test}}$, we applied the controller with the closest training task $\boldsymbol{\eta}^{\text{train}}$.

Re-weighted independent controllers (RW-IC): Training was identical to NN-IC. At test time, we combined individual controllers using a gating network, similar to [22], resulting in a convex combination of local policies. The gating-network weights were

$$v_i = \frac{\exp\left(-\frac{1}{2\kappa}\|\boldsymbol{\eta}^{\text{test}} - \boldsymbol{\eta}_i^{\text{train}}\|^2\right)}{\sum_j |\boldsymbol{\eta}_j^{\text{train}}| \exp\left(-\frac{1}{2\kappa}\|\boldsymbol{\eta}^{\text{test}} - \boldsymbol{\eta}_j^{\text{train}}\|^2\right)}, \quad (10)$$

such that the applied control signal was $\mathbf{u} = \sum_i v_i \pi_i(\mathbf{x})$. An extensive grid search resulted in $\kappa = 0.0068 \text{ m}^2$, leading to the best test performance in this scenario, making RW-IC nearly identical to the NN-IC.

Multi-task policy search, $\boldsymbol{\Sigma}^\eta = \mathbf{0}$ (MTPS0): Multi-task policy search with five known tasks during training, which only differ in the location of the cart where the pendulum is supposed to be balanced. The target locations were $\boldsymbol{\eta}^{\text{train}} = \{\pm 1 \text{ m}, \pm 0.5 \text{ m}, 0 \text{ m}\}$. Moreover, $g(\mathbf{x}_t, \boldsymbol{\eta}) = \boldsymbol{\eta} - \chi(t)$ and $\boldsymbol{\Sigma}^\eta = \mathbf{0}$. We show results after 20 trials, i.e., a total experience of 70 s only.

Multi-task policy search, $\boldsymbol{\Sigma}^\eta > \mathbf{0}$ (MTPS+): Multi-task policy search with the five training tasks $\boldsymbol{\eta}^{\text{train}} = \{\pm 1 \text{ m}, \pm 0.5 \text{ m}, 0 \text{ m}\}$, but with training task covariance $\boldsymbol{\Sigma}^\eta = \text{diag}([0.1^2, 0, 0, 0])$. We show results after 20 trials, i.e., 70 s total experience.

For testing the performance of the algorithms, we applied the learned policies 100 times to the test-target locations $\eta^{\text{test}} = -1.5, -1.4, \dots, 1.5$. Every time, the initial state of a rollout was sampled from $p(\mathbf{x}_0)$. For the MTPS experiments, we plugged the test tasks into Eq. (2) to compute the corresponding control signals.

Fig. 4 illustrates the generalization performance of the learned controllers. The horizontal axes denote the locations η^{test} of the target position of the cart at *test* time. The height of the bars show the average (over trials) cost per time step. The means of the *training* tasks η^{train} are the location of the red bars. For Experiment 1, Fig. 4(d) shows the distribution $p(\eta_i^{\text{train}})$ used during training as the bell-curves, which approximately covers the range $\eta \in [-1.2 \text{ m}, 1.2 \text{ m}]$.

The NN-IC controller in the nearest-neighbor baseline, see Fig. 4(a), balanced the pendulum at a cart location that was not further away than 0.2 m, which incurred a cost of up to 0.45. In Fig. 4(b), the performances for the hierarchical RW-IC controller are shown. The performance for the best value κ in the gating network, see Eq. (10), was similar to the performance of the NN-IC controller. However, between the training tasks for the local controllers, where the test tasks were in the range of $[-0.9 \text{ m}, 0.9 \text{ m}]$, the convex combination of local controllers led to more failures than in NN-IC, where the pendulum could not be swung up successfully: Convex combinations of nonlinear local controllers eventually decreased the (non-existing) generalization performance of RW-IC.

Fig. 4(c) shows the performance of the MTPS0 controller. The MTPS0 controller successfully performed the swing-up plus balancing task for all tasks η^{test} close to the training tasks. However, the performance varied relatively strongly. Fig. 4(d) shows that the MTPS+ controller successfully performed the swing-up plus balancing task for all tasks η^{test} at test time that were sufficiently covered by the uncertain training tasks $\eta_i^{\text{train}}, i = 1, \dots, 5$, indicated by the bell curves representing $\Sigma^\eta > 0$. Relatively constant performance across the test tasks covered by the bell curves was achieved. An average cost of 0.3 meant that the pendulum might be balanced with the cart slightly offset. Fig. 2 shows the learned MTPS+ policy for all test tasks η^{test} with the state $\mathbf{x} = \mu_0$ fixed.

Tab. I summarizes the expected costs across all test tasks η^{test} . We averaged over all test tasks and 100 applications of the learned policy, where the initial state was sampled from $p(\mathbf{x}_0)$. Although NN-IC and RW-IC performed swing-up reliably, they incurred the largest cost: For most test tasks, they balanced the pendulum at the wrong cart position as they could not generalize from training tasks to unseen test tasks. In the MTPS experiments, the average cost was lowest, indicating that our multi-task policy search approach

TABLE I
MULTI-TASK CART-POLE SWING-UP: AVERAGE COSTS ACROSS 31 TEST TASKS η^{TEST} .

	NN-IC	RW-IC	MTPS0	MTPS+
Cost	0.39	0.4	0.33	0.30

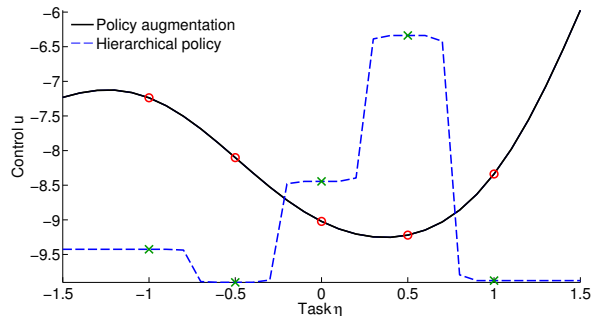


Fig. 5. Two multi-task policies for a given state \mathbf{x} , but varying task η . The black policy is obtained by applying our proposed multi-task approach (MTPS+); the blue, dashed policy is obtained by hierarchically combining local controllers (RW-IC). The training tasks are $\eta = \{\pm 1, \pm 0.5, 0\}$. The corresponding controls $u = \pi(\mathbf{x}, \eta)$ are marked by the red circles (MTPS+) and the green stars (RW-IC), respectively. MTPS+ generalizes more smoothly across tasks, whereas the hierarchical combination of independently trained local policies does not generalize well.

is beneficial. MTPS+ led to the best overall generalization performance, although it might not solve each individual test task optimally.

Fig. 5 illustrates the difference in generalization performance between our MTPS+ approach and the RW-IC approach, where controls u_i from local policies π_i are combined by means of a gating network. Since the local policies are trained independently, a (convex) combination of local controls makes only sense in special cases, e.g., when the local policies are linear in the parameters. In this example, however, the local policies are nonlinear. Since the local policies are learned independently, their overall generalization performance is poor. On the other hand, MTPS+ learns a single policy for a task η_i always in the light of all other tasks $\eta_j \neq i$ as well, and, therefore, leads to an overall smooth generalization.

B. Multi-Task Robot Manipulator

Our proposed multi-task learning method has been applied to a block-stacking task using a low-cost, off-the-shelf robotic manipulator (\$370) by Lynxmotion [1], see Fig. 6(a), and a PrimeSense [2] depth camera (\$130) used as a visual sensor. The arm had six controllable degrees of freedom: base rotate, three joints, wrist rotate, and a gripper (open/close). The plastic arm could be controlled by commanding both a desired configuration of the six servos (via their pulse durations) and the duration for executing the command [14]. The camera was identical to the Kinect sensor, providing a synchronized depth image and a 640×480 RGB image at 30 Hz. We used the camera for 3D-tracking of the block in the robot’s gripper.

The goal was to make the robot learn to stack a tower of six blocks using multi-task learning. The cost function c in Eq. (1) penalized the distance of the block in the gripper from the desired drop-off location. We only specified the 3D camera coordinates of the blocks B2, B4, and B5 as the training tasks η^{train} , see Fig. 6(a). Thus, at test time, stacking B3 and B6 required exploiting the generalization of

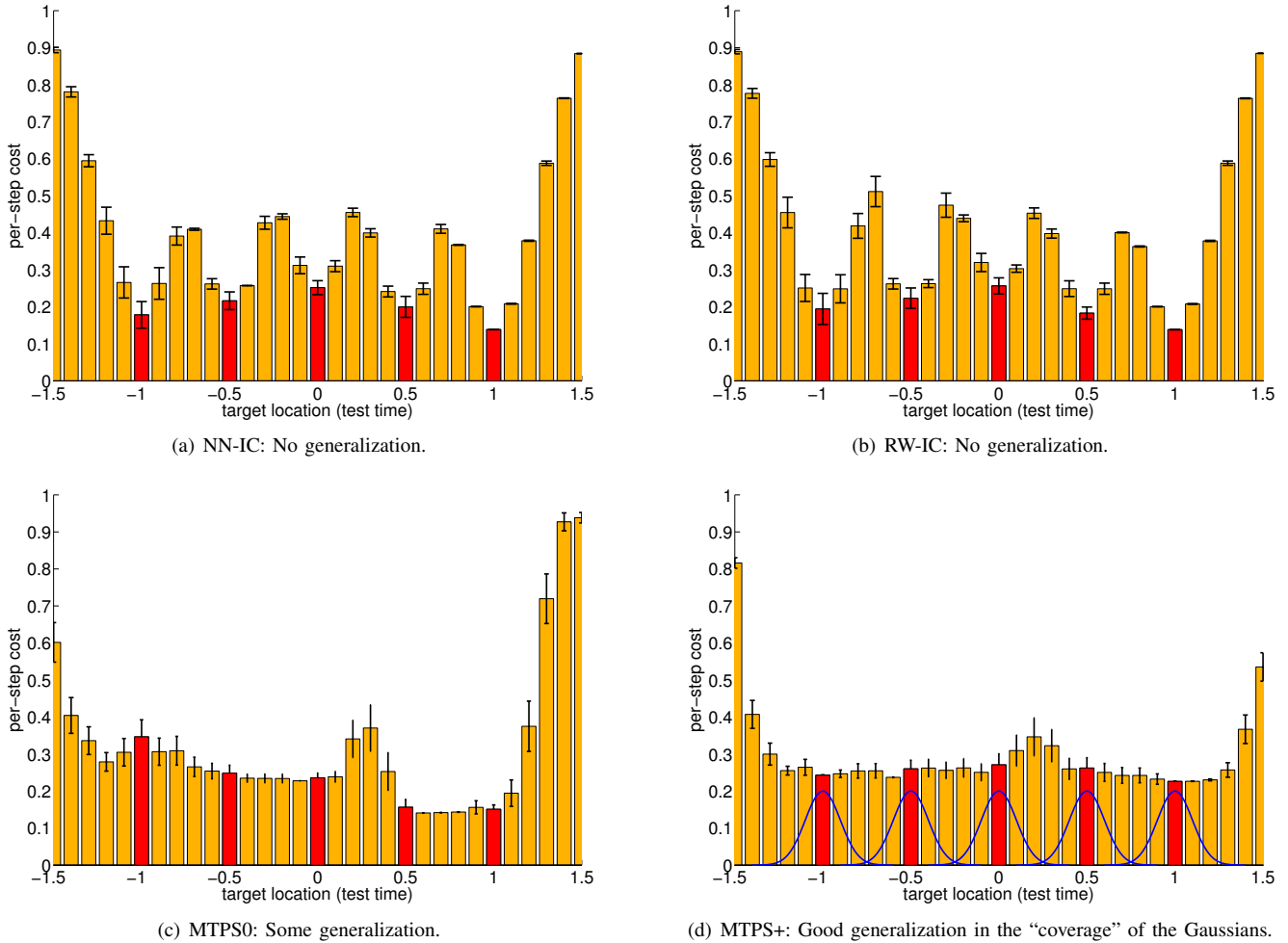


Fig. 4. Generalization performance for the multi-task cart-pole swing-up. The graphs show the expected cost per time step along with twice the standard errors.

the multi-task policy search. We chose $g(x, \eta) = \eta - x$. Moreover, we set Σ^η such that the task space, i.e., all 6 blocks, was well covered. The mean μ_0 of the initial distribution $p(x_0)$ corresponded to an upright configuration of the arm.

A GP dynamics model was learned that mapped the 3D camera coordinates of the block in the gripper and the commanded controls at time t to the corresponding 3D coordinates of the block in the gripper at time $t + 1$, where the control signals were changed at a rate of 2 Hz. Note that the learned model is not an inverse kinematics model as the robot’s joint state is unknown. We used an affine policy $u_t = \pi(x_t, \eta, \theta) = Ax_t^{x, \eta} + b$, where $\theta = \{A, b\}$. The policy now defined a mapping $\pi : \mathbb{R}^6 \rightarrow \mathbb{R}^4$, where the four controlled degrees of freedom were the base rotate and three joints.

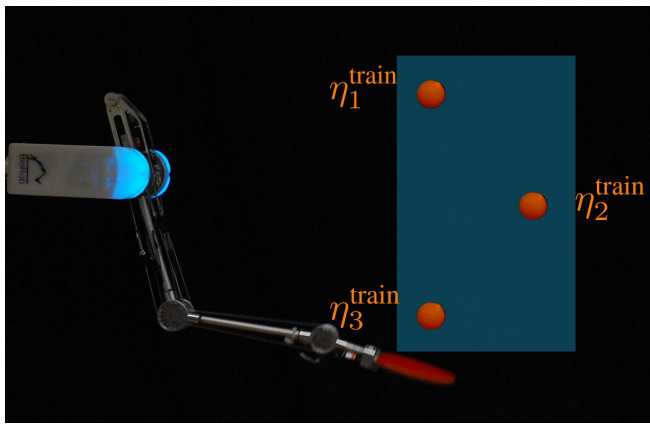
We report results based on 16 training trials, each of length 5 s, which amounts to a total experience of 80 s only. The test phase consisted of 10 trials per stacking task, where the arm was supposed to stack the block on the currently topmost block. The tasks η_j^{test} at test time corresponded to stacking blocks B2–B6 in Fig. 6(a).

Fig. 6(b) shows the average distance of the block in the

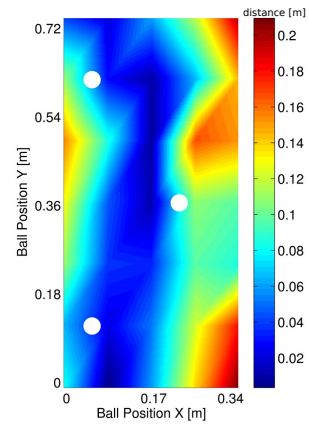
gripper from the target position, which was $b = 4.3$ cm above the topmost block. Here, “block2” means that the task was to move block B2 in the gripper on top of block 1. The horizontal axis shows times at which the manipulator’s control signal was changed (rate 2 Hz), the vertical axis shows the average distances (over 10 test trials) to the target position in meters. For all blocks (including blocks B3 and B6, which were not part of the training tasks η^{train}) the distances approached zero over time. Thus, the learned multi-task controller was able to interpolate (block B3) and extrapolate (block B6) from the training tasks to the test tasks *without* re-training.

C. Multi-Task Imitation Learning of Ball-Hitting Movements

We demonstrate that our MTPS approach can also be applied to imitation learning. Instead of defining a cost function c in Eq. (1), a teacher provides demonstrations that the robot should imitate. We show that our MTPS approach allows to generalize from demonstrated behavior to behaviors that have not been observed before. In [15], we developed a method for model-based imitation learning based on probabilistic trajectory matching for a single task. The key idea is to match a distribution over predicted robot trajectories $p(\tau^\pi)$ directly

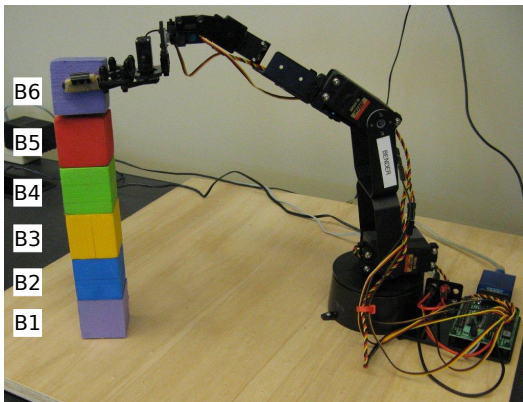


(a) Set-up for the imitation learning experiments. The orange balls represent the three training tasks η_j^{train} . The blue rectangle indicates the regions of the test tasks η_j^{test} for our learned controller to which we want to generalize.

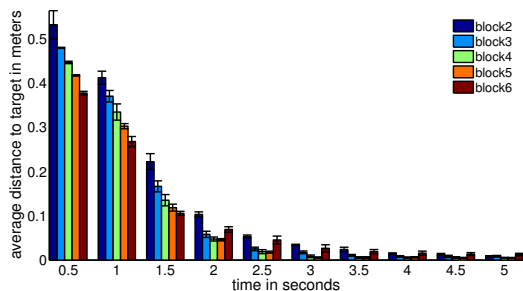


(b) The white discs are the training task locations. Blue and cyan indicate that the task was solved successfully.

Fig. 7. Set-up and results for the imitation learning experiments with a bio-inspired BioRob™.



(a) Low-cost manipulator by Lynxmotion [1] performing a block-stacking task.



(b) Average distances of the block in the gripper from the target position (with twice the standard error).

Fig. 6. Experimental setup and results for the multi-task block-stacking task. A controller was learned directly in the task space using visual feedback from a PrimeSense depth camera.

with an observed distribution $p(\tau^{\text{exp}})$ over expert trajectories τ^{exp} by finding a policy π^* that minimizes the KL divergence [28] between them.

In this paper, we extend this imitation learning approach to a multi-task scenario to jointly learning to imitate multiple tasks from a small set of demonstrations. In particular, we applied our multi-task learning approach to learning a controller for hitting movements with variable ball positions in a

2D-plane using the tendon-driven BioRob™ X4, a five DoF compliant, light-weight robotic arm, capable of achieving high accelerations, see Fig. 7(a). The torques are transferred from the motor to the joints via a system of pulleys, drive cables, and springs, which, in the biomechanically-inspired context, represent tendons and their elasticity. While the BioRob’s design has advantages over traditional approaches, modeling and controlling such a compliant system is challenging.

In our imitation-learning experiment, we considered three joints of the robot, such that the state $\mathbf{x} \in \mathbb{R}^6$ contained the joint positions \mathbf{q} and velocities $\dot{\mathbf{q}}$ of the robot. The controls $\mathbf{u} \in \mathbb{R}^3$ were given by the corresponding motor torques, directly determined by the policy π . For learning a controller, we used an RBF network with 250 Gaussian basis functions, where the policy parameters comprised the locations of the basis functions, their weights, and a shared diagonal covariance matrix, resulting in about 2300 policy parameters. Policy learning required about 20 minutes computation time. Unlike in the previous examples, we represented a task as a two-dimensional vector $\eta \in \mathbb{R}^2$ corresponding to the ball position in Cartesian coordinates in an arbitrary reference frame within the hitting plane. As the task representation η was basically an index and, hence, unrelated to the state of the robot, $g(\mathbf{x}, \eta) = \eta$, and the cross-covariances $C^{x\eta}$ in Eq. (2) were $\mathbf{0}$.

As training tasks η_j^{train} , we defined hitting movements for three different ball positions, see Fig. 7(a). For each training task, an expert demonstrated two hitting movements via kinesthetic teaching. Our goal was to learn a single policy that a) learns to imitate three distinct expert demonstrations, and b) generalizes from demonstrated behaviors to tasks that were not demonstrated. In particular, these tests tasks were defined as hitting balls in a larger region around the training locations, indicated by the blue box in Fig. 7(a). We set the matrices Σ^η such that the blue box was covered well.

Fig. 7(b) shows the performance results as a heatmap after 15 iterations of Alg. 3. The evaluation measure was the

distance in m between the ball position and the center of the table-tennis racket. We computed this error in a regular 7x5 grid of the blue area in Fig. 7(a). The distances in the blue and cyan areas were sufficient to successfully hit the ball (the racket’s radius is about 0.08 m). Hence, our approach successfully generalized from given demonstrations to new tasks that were not in the library of demonstrations.

D. Remarks

Controlling the cart-pole system to different target location is a task that could be solved without the task-augmentation of the controller inputs: It is possible to learn a controller that depends only on the position of the cart relative to the target location—the control signals should be identical when the cart is at location χ , the target location is at $\chi + \varepsilon$ or when the cart is at location at position x_2 , and the target location is at $x_2 + \varepsilon$. Our approach, however, learns these invariances automatically, i.e., it does not require an intricate knowledge of the system/controller properties. Note that a linear combination of local controllers usually does not lead to success in the cart-pole system, which requires a nonlinear controller for the joint task of swinging up the pendulum and balancing it in the inverted position.

In the case of the Lynx-arm, these invariances no longer exist as the optimal control signal depends on the absolute position of the arm, not only on the relative distance to the target. Since a linear controller is sufficient to learn block stacking, a convex combination of individual controllers should be able to generalize from the trained blocks to new targets if no extrapolation is required.

IV. CONCLUSION AND FUTURE WORK

We have presented a policy-search approach to multi-task learning for robots, where we assume stationary dynamics. Instead of combining local policies using a gating network, which only works for linear-in-the-parameters policies, our approach learns a single policy jointly for all tasks. The key idea is to explicitly parametrize the policy by the task and, therefore, enable the policy to generalize from training tasks to similar, but unknown, tasks at test time. This generalization is phrased as an optimization problem, jointly with learning the policy parameters. For solving this optimization problem, we incorporated our approach into the PILCO policy search framework, which allows for data-efficient policy learning. We have reported promising results on multi-task RL on a standard benchmark problem and on a robotic manipulator. Our approach also applies to imitation learning and generalizes imitated behavior to solving tasks that were not in the library of demonstrations.

In this paper, we considered the case that re-training the policy after a test run is not allowed. Relaxing this constraint and incorporating the experience from the test trials into a subsequent iteration of the learning procedure would improve the average quality of the controller.

In future, we will jointly learn the task representation for the policy and the policy parametrization. Thereby, it will not be necessary to specify any interdependence between

task and state space a priori, but this interdependence will be learned from data.

REFERENCES

- [1] <http://www.lynxmotion.com>.
- [2] <http://www.primesense.com>.
- [3] P. Abbeel and A. Y. Ng. Exploration and Apprenticeship Learning in Reinforcement Learning. In *ICML*, 2005.
- [4] P. Abbeel, M. Quigley, and A. Y. Ng. Using Inaccurate Models in Reinforcement Learning. In *ICML*, 2006.
- [5] C. G. Atkeson and J. C. Santamaria. A Comparison of Direct and Model-Based Reinforcement Learning. In *ICRA*, 1997.
- [6] J. A. Bagnell and J. G. Schneider. Autonomous Helicopter Control using Reinforcement Learning Policy Search Methods. In *ICRA*, 2001.
- [7] S. Barrett, M. E. Taylor, and P. Stone. Transfer Learning for Reinforcement Learning on a Physical Robot. In *AAMAS*, 2010.
- [8] B. C. da Silva, G. Konidaris, and A. G. Barto. Learning Parametrized Skills. In *ICML*, 2012.
- [9] M. P. Deisenroth. *Efficient Reinforcement Learning using Gaussian Processes*. KIT Scientific Publishing, 2010. ISBN 978-3-86644-569-7.
- [10] M. P. Deisenroth, P. Englert, J. Peters, and D. Fox. Multi-Task Policy Search for Robotics. In *ICRA*, 2014.
- [11] M. P. Deisenroth, D. Fox, and C. E. Rasmussen. Gaussian Processes for Data-Efficient Learning in Robotics and Control. *IEEE-TPAMI*, 2014.
- [12] M. P. Deisenroth, G. Neumann, and J. Peters. *A Survey on Policy Search for Robotics*, volume 2 of *Foundations and Trends in Robotics*. NOW Publishers, 2013.
- [13] M. P. Deisenroth and C. E. Rasmussen. PILCO: A Model-Based and Data-Efficient Approach to Policy Search. In *ICML*, 2011.
- [14] M. P. Deisenroth, C. E. Rasmussen, and D. Fox. Learning to Control a Low-Cost Manipulator using Data-Efficient Reinforcement Learning. In *RSS*, 2011.
- [15] P. Englert, A. Paraschos, J. Peters, and M. P. Deisenroth. Model-based Imitation Learning by Probabilistic Trajectory Matching. In *ICRA*, 2013.
- [16] A. J. Ijspeert, J. Nakanishi, and S. Schaal. Learning Attractor Landscapes for Learning Motor Primitives. In *NIPS*, 2002.
- [17] R. A. Jacobs, M. I. Jordan, S. J. Nowlan, and G. E. Hinton. Adaptive Mixtures of Local Experts. *Neural Computation*, 3:79–87, 1991.
- [18] J. Ko, D. J. Klein, D. Fox, and D. Haehnel. Gaussian Processes and Reinforcement Learning for Identification and Control of an Autonomous Blimp. In *ICRA*, 2007.
- [19] J. Kober, A. Wilhelm, E. Oztop, and J. Peters. Reinforcement Learning to Adjust Parametrized Motor Primitives to New Situations. *Autonomous Robots*, 33(4):361–379, 2012.
- [20] G. Konidaris, I. Scheidwasser, and A. G. Barto. Transfer in Reinforcement Learning via Shared Features. *JMLR*, 13:1333–1371, 2012.
- [21] O. Kroemer, R. Detry, J. Piater, and J. Peters. Combining Active Learning and Reactive Control for Robot Grasping. *Robotics and Autonomous Systems*, 58:1105–1116, 2010.
- [22] K. Mülling, J. Kober, O. Kroemer, and J. Peters. Learning to Select and Generalize Striking Movements in Robot Table Tennis. *IJRR*, 2013.
- [23] J. Peters and S. Schaal. Policy Gradient Methods for Robotics. In *IRIS*, 2006.
- [24] J. Quiñero-Candela, A. Girard, J. Larsen, and C. E. Rasmussen. Propagation of Uncertainty in Bayesian Kernel Models—Application to Multiple-Step Ahead Forecasting. In *ICASSP*, 2003.
- [25] C. E. Rasmussen and C. K. I. Williams. *Gaussian Processes for Machine Learning*. The MIT Press, 2006.
- [26] S. Schaal. Learning From Demonstration. In *NIPS*. 1997.
- [27] J. G. Schneider. Exploiting Model Uncertainty Estimates for Safe Dynamic Control Learning. In *NIPS*. 1997.
- [28] K. Solomon. *Information Theory and Statistics*. Wiley, New York, 1959.
- [29] R. S. Sutton and A. G. Barto. *Reinforcement Learning: An Introduction*. The MIT Press, 1998.
- [30] M. E. Taylor and P. Stone. Cross-Domain Transfer for Reinforcement Learning. In *ICML*, 2007.
- [31] M. E. Taylor and P. Stone. Transfer Learning for Reinforcement Learning Domains: A Survey. *JMLR*, 10(1):1633–1685, 2009.